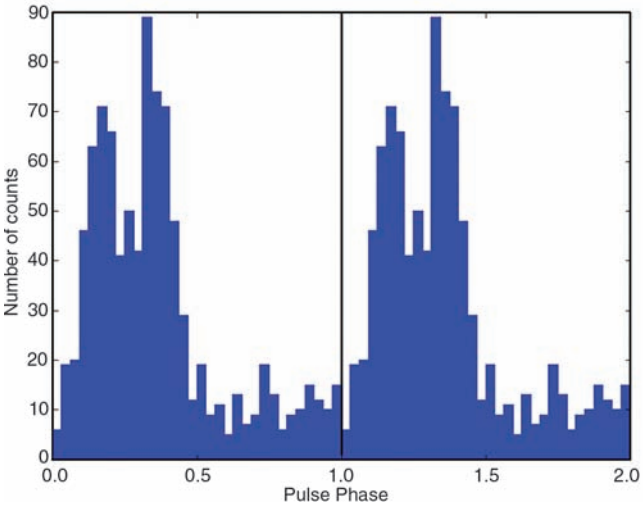

Fig. 3. Gamma-ray (>100 MeV) light-curve of the pulsar in CTA 1 shown over two periods of rotation with a resolution of 32 phase bins per period (corresponding to ~10 ms per bin). The two maxima in the broad emission feature each have a full width at half maximum of ~0.12 and are separated by ~0.2 in phase. Overall, the LAT pulsar light-curve is similar to the gamma-ray light-curve of the *EGRET* pulsar PSR B1706-44 (*23*).

References and Notes

1. D. E. Harris, J. A. Roberts, *Publ. Astron. Soc. Pac.* **72**, 237 (1960).
2. D. E. Harris, *Astrophys. J.* **135**, 661 (1962).
3. J. L. Caswell, *Mon. Not. R. Astron. Soc.* **136**, 11 (1967).
4. W. Sieber, C. G. T. Haslam, C. J. Salter, *Astron. Astrophys.* **74**, 361 (1979).
5. W. Sieber, C. J. Salter, C. J. Mayer, *Astron. Astrophys.* **103**, 393 (1981).
6. S. Pineault *et al.*, *Astron. J.* **105**, 1060 (1993).
7. S. Pineault *et al.*, *Astron. Astrophys.* **324**, 1152 (1997).
8. F. Mavromatakis *et al.*, *Astron. Astrophys.* **353**, 371 (2000).
9. P. Slane *et al.*, *Astrophys. J.* **485**, 221 (1997).
10. P. Slane *et al.*, *Astrophys. J.* **601**, 1045 (2004).
11. F. D. Seward, B. Schmidt, P. Slane, *Astrophys. J.* **453**, 284 (1995).
12. J. P. Halpern *et al.*, *Astrophys. J.* **612**, 398 (2004).
13. R. C. Hartman *et al.*, *Astrophys. J.* **123** (suppl.), 79 (1999).
14. K. T. S. Brazier *et al.*, *Mon. Not. R. Astron. Soc.* **295**, 819 (1998).
15. S. J. Sturner, C. D. Dermer, J. Mattox, *Astron. Astrophys.* **120** (suppl.), 445 (1996).
16. P. F. Michelson *et al.*, *Proceedings of 1st GLAST Symposium*, S. Ritz, P. Michelson, C. Meegan, Eds. (American Institute of Physics, New York, 2007).
17. W. B. Atwood *et al.*, *Astrophys. J.* **652**, L49 (2006).
18. S. M. Ransom, thesis, Harvard University (2001), available at http://www.cv.nrao.edu/~sransom/presto/.
19. G. B. Hobbs, R. T. Edwards, R. N. Manchester, *Not. R. Astron. Soc.* **369**, 655 (2006).
20. D. A. Smith *et al.*, *Astron. Astrophys.*, in press; preprint available at http://adsabs.harvard.edu/abs/2008arXiv0810.1637S.
21. Extrapolation of the present pulsar ephemeris back to the archival epochs results in a large range of uncertainty for the period. Searches in *XMM* data by members of the Fermi LAT collaboration are not yet conclusive.
22. T. Gold, *Nature* **221**, 25 (1969).
23. D. J. Thompson *et al.*, *Astrophys. J.* **465**, 385 (1996).
24. K. Hirotani, preprint available at http://arxiv.org/abs/0809.1283v1 (2008).
25. A. K. Harding, J. V. Stern, J. Dyks, M. Frackowiak, *Astrophys. J.* **680**, 1378 (2008).
26. R. W. Romani, I. A. Yadigaroglu, *Astrophys. J.* **438**, 314 (1995).
27. M. G. Baring, *Adv. Space Res.* **33**, 552 (2004).
28. R. W. Romani, *Astrophys. J.* **470**, 469 (1996).
29. G. Kanbach *et al.*, *Astron. Astrophys.* **120** (suppl.), 461 (1996).
30. G. Hobbs *et al.*, *Mon. Not. R. Astron. Soc.* **360**, 974 (2005).
31. The Fermi LAT Collaboration acknowledges the generous support of a number of agencies and institutes, including NASA and the U.S. Department of Energy in the United States; the Commissariat l'Energie Atomique and the Centre National de la Recherche Scientifique/Institut National de Physique Nuclaire et de Physique des Particules in France; the Agenzia Spaziale Italiana and the Istituto Nazionale di Fisica Nucleare in Italy; the Ministry of Education, Culture, Sports, Science and Technology, the High Energy Accelerator Research Organization, and JAXA in Japan, and the K. A. Wallenberg Foundation and the Swedish National Space Board in Sweden.

Supporting Online Material

www.sciencemag.org/cgi/content/full/1165572/DC1
Fig. S1

5 September 2008; accepted 8 October 2008
Published online 16 October 2008;
10.1126/science.1165572
Include this information when citing this paper.

Observation of Pulsed γ-Rays Above 25 GeV from the Crab Pulsar with MAGIC

The MAGIC Collaboration*

One fundamental question about pulsars concerns the mechanism of their pulsed electromagnetic emission. Measuring the high-end region of a pulsar's spectrum would shed light on this question. By developing a new electronic trigger, we lowered the threshold of the Major Atmospheric γ-ray Imaging Cherenkov (MAGIC) telescope to 25 giga–electron volts. In this configuration, we detected pulsed γ-rays from the Crab pulsar that were greater than 25 giga–electron volts, revealing a relatively high cutoff energy in the phase-averaged spectrum. This indicates that the emission occurs far out in the magnetosphere, hence excluding the polar-cap scenario as a possible explanation of our measurement. The high cutoff energy also challenges the slot-gap scenario.

It is generally accepted that the primary radiation mechanism in pulsar magnetospheres is synchrotron-curvature radiation. This occurs when relativistic electrons are trapped along the magnetic field lines in the extremely strong field of the pulsar. Secondary mechanisms include ordinary synchrotron and inverse Compton scattering. It is not known whether the emission of electromagnetic radiation takes place closer to the neutron star (NS) [the polar-cap scenario (*1*–*3*)] or farther out in the magnetosphere [the slot-gap (*4*–*6*) or outer-gap (*7*–*9*) scenario (Fig. 1)]. The high end of the γ-ray spectrum differs substantially between the near and the far case. Moreover, current models of the slot gap (*6*) and the outer gap (*8*, *9*) differ in their predicted γ-ray spectra, even though both gaps extend over similar regions in the magnetosphere. Therefore, detection of γ-rays above 10 GeV would allow one to discriminate between different pulsar emission models.

At gamma-ray energies (E) of ~1 GeV, some pulsars such as the Crab (PSR B0531+21) are among the brightest γ-ray sources in the sky. The Energetic γ-ray Experiment Telescope (EGRET) detector, aboard the Compton γ-ray Observatory (CGRO), measured the γ-ray spectra of different pulsars only up to $E \approx 5$ GeV because of its small detector area (~0.1 m^2) and the steeply falling γ-ray fluxes at higher energies. At $E > 60$ GeV, Cherenkov telescopes (*10*) are the most sensitive instruments because of their large detection areas of $\geq 10^4$ m^2. But, in spite of several attempts, no pulsar has yet been detected at such energies (*11*–*16*). This suggests a spectral cutoff; that is, that the pulsar's emission drops off sharply, between a few giga–electron volts and a few tens of giga–electron volts.

The Crab pulsar is one of the best candidates for studying such a cutoff. Its spectrum has been measured by EGRET (*17*) up to $E \approx 5$ GeV without a clear cutoff being seen. Earlier observations with the 17-m-diameter Major Atmospheric γ-ray Imaging Cherenkov (MAGIC) (*18*) telescope (Canary Island of La Palma, 2200 m above sea level) revealed a hint of pulsed emission at the 2.9 standard deviation (σ) level above 60 GeV (*19*, *20*). To verify this result, we developed and installed a new trigger system that lowered the threshold of MAGIC from ~50 GeV to 25 GeV [supporting online material (SOM) text] (*21*).

We observed the Crab pulsar between October 2007 and February 2008, obtained 22.3 hours of good-quality data, and detected pulsed emission above 25 GeV. The pulsed signal (Fig. 2) has an

*The full list of authors and affiliations is presented at the end of this paper.

overall significance of 6.4 σ with 8500 ± 1330 signal events. Phase zero (ϕ = 0) is defined as the position of the main radio pulse (*22*). Our $E >$ 25 GeV data show pronounced pulses at ϕ = 0 (main pulse, P1) and at ϕ = 0.3 to 0.4 (interpulse, P2). These pulses are coincident with those measured by EGRET at $E >$ 100 MeV and those coming from our own optical measurement. P1 and P2 have similar amplitudes at E = 25 GeV, in contrast to measurements at lower energies of $E >$ 100 MeV, at which P1 is dominant. The present data show a small excess (3.4 σ) above 60 GeV for P2, which is consistent with our previous Crab observation (*19*, *20*).

For the Crab pulsar, EGRET measured a power-law spectrum [$F(E) \propto E^{-\alpha}$ with a spectral index α = 2.022 ± 0.014 and F is the flux] in the energy range from E = 0.1 GeV to 5 GeV (*17*). At E = 25 GeV we measured a flux that was several times lower than a straightforward extrapolation of the EGRET spectrum, which would require a spectral cutoff of somewhere between 5 and 25 GeV. Pulsar emission scenarios predict a generalized exponential shape for the cutoff that may be described as $F(E) = AE^{-\alpha}\exp[-(E/E_0)^{\beta}]$, where A is a normalized constant, E_0 is the cutoff energy, and β measures the steepness of the cutoff. To determine the relevant parameters, we performed a joint fit to the Imaging Compton Telescope (COMPTEL) (≈1 to 30 MeV), EGRET (≈30 MeV to 10 GeV), and MAGIC (>25 GeV) data. For the conventional cases of β = 1 (exponential) and β = 2 (super-exponential), we found $E_0 = 17.7 \pm 2.8_{stat} \pm 5.0_{syst}$ GeV (stat, statistical error; syst, systematic error) and $E_0 = 23.2 \pm 2.9_{stat} \pm 6.6_{syst}$ GeV, respectively (Fig. 3). When β is left as a free parameter, the best fit yields $E_0 = 20.4 \pm 3.9_{stat} \pm 7.4_{syst}$ GeV and β = 1.2. The systematic error is dominated by a possible mismatch between the energy calibrations of EGRET and MAGIC (SOM text).

From a theoretical point of view, the spectral cutoff is explained as a combination of the maximum energies that electrons (e) can reach (because of the balance between acceleration and radiation losses) and the absorption of the emitted γ-rays in the magnetosphere. Absorption is controlled by two mechanisms: (i) magnetic e^+-e^- pair production in the extremely strong magnetic field close to the pulsar surface and (ii) photon-photon e^+-e^- pair production in dense photon fields. If, for a young pulsar like the Crab with a magnetic field $B \sim 10^{12}$ to 10^{13} G, emission occurs close to the NS surface [as in classical polar-cap models (*1*–*3*)], then magnetic pair-production attenuation provides a characteristic super-exponential cutoff at relatively low energies; that is, a few giga–electron volts at most (*3*). If, on the other hand, emission occurs farther out in the magnetosphere, at several stellar radii or close to the light cylinder [as in slot-gap (*4*–*6*) and outer-gap (*7*–*9*, *23*) models], then absorption mainly arising from photon-photon collisions sets in at higher energies and produces a shallower cutoff (roughly exponential in shape). In either case, however, the measured E_0 could be intrinsic to the emitted spectrum and hence would only provide an upper limit to the absorption strength.

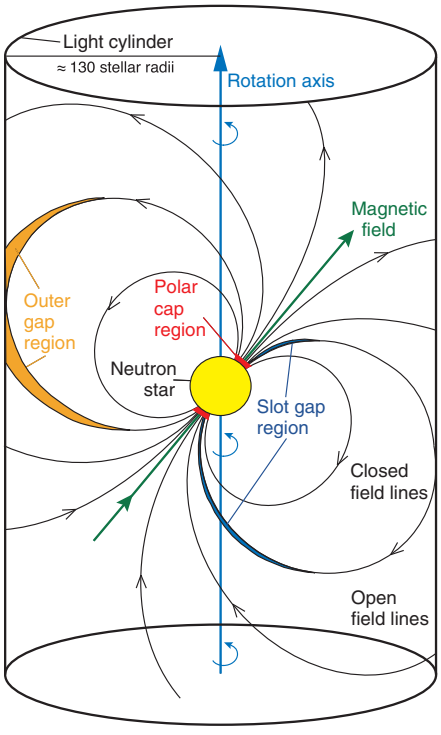

Fig. 1. A sketch of the Crab pulsar's magnetosphere. Electrons are trapped and accelerated along the magnetic field lines of the pulsar and emit electromagnetic radiation via the synchrotron-curvature mechanism. Vacuum gaps or vacuum regions occur at the polar cap (*1*–*3*) very close to the neutron star surface in a thin layer extending for several stellar radii along the boundary of the closed magnetosphere, the so-called slot gap (*4*–*6*), and in the outer region (*7*–*9*) close to the light cylinder (the outer gap). Vacuum gaps are filled with plasma, but its density is lower than the critical Goldreich-Julian density (*24*), in which the magnetically induced electric field is saturated, and therefore electrons can be accelerated to very high energies. Absorption of high-energy γ-rays occurs by interaction with the magnetic field (magnetic pair production) as well as with the photon field (photon-photon pair production). The former dominates close to the surface of the neutron star where the magnetic field is strongest; it leads to a superexponential cutoff at relatively low energies (few giga–electron volts). Photon-photon collisions prevail farther out in the magnetosphere close to the light cylinder, where the magnetic field is lower, and lead to a roughly exponential cutoff at higher (>10 GeV) energies.

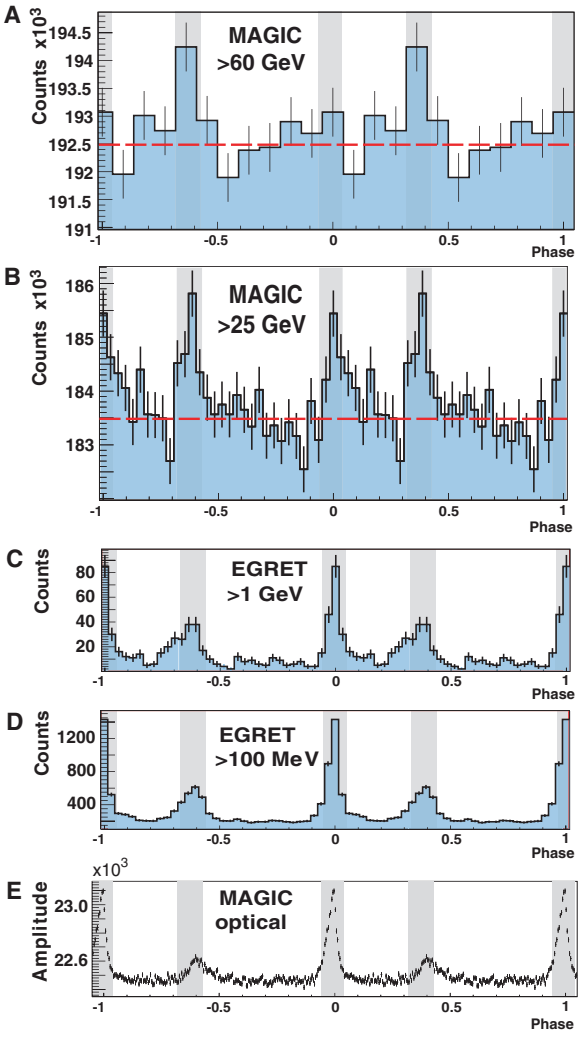

Fig. 2. Pulsed emission in different energy bands. The shaded areas show the signal regions for P1 and P2. (**A**) Evidence of an emission (3.4 σ) greater than 60 GeV for P2, measured by MAGIC. (**B**) Emission ≥ 25 GeV, measured by MAGIC. (**C**) Emission ≥1 GeV, measured by EGRET (*17*). (**D**) Emission ≥ 100 MeV, measured by EGRET (*25*). (**E**) Optical emission measured by MAGIC with the central pixel (*26*) of the camera. The optical signal has been recorded simultaneously with the γ-rays. P1 and P2 are in phase for all shown energies. The ratio of P2/P1 increases with energy from (B) to (D). In the search for a pulsed emission, the arrival time of each event, after correcting for the solar system barycenter, was transformed into the phase of the rotational period of the neutron star. The significance of the γ-ray pulsation greater than 25 GeV was evaluated by a single-hypothesis test (SOM text), in which the γ-ray emission was assumed to be coming from the two fixed phase intervals (shaded regions): P1 (phase 0.94 to 0.04) and P2 (phase 0.32 to 0.43), as defined in (*19*, *20*). The signal results in 8500 ± 1330 signal events (6.4 σ).

Equation 1 of (*3*) (a largely model-independent relation derived from simulations of γ-ray absorption by magnetic-pair production in rotating magnetic dipoles) relates the pair-creation cutoff energy, E_{max}, with the location of the emission region r/R_0 (R_0 is the NS radius; r is the distance of the emission region from the center of the NS) for a NS with surface magnetic field B_0 and period P:

$$E_{max} \approx 0.4\sqrt{P\frac{r}{R_0}}\max\left\{1, \frac{0.1B_{crit}}{B_0}\left(\frac{r}{R_0}\right)^3\right\}\text{GeV} \quad (1)$$

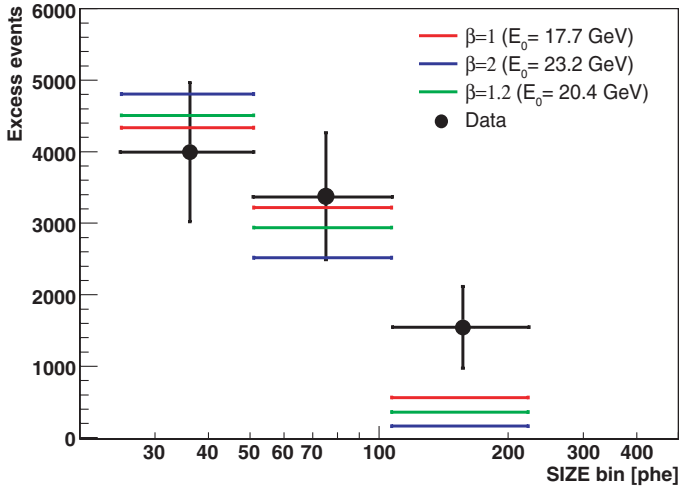

Fig. 3. Model fits to the signal-event distribution. Shown is the measured distribution of excess events in bins of *SIZE* integrated over P1 and P2. *SIZE* is a main image parameter that measures the total intensity of the Cherenkov flash in the camera in units of photoelectrons (phe). In this analysis, it was used as a rough estimate of the γ-ray energy. To determine the cutoff energy, we folded the power law function with the generalized exponential shape function $F(E) = AE^{1\alpha}\exp[-(E/E_0)^{\beta}]$ with the MAGIC telescope's effective area to calculate the expected signal in each *SIZE* bin (forward unfolding). The expected signal was compared with the measured excess events by calculating a χ^2 test. We obtained the best fit by minimizing the joint χ^2 between real data (from COMPTEL, EGRET, and MAGIC) and the generalized function $F(E) = AE^{1\alpha}\exp[-(E/E_0)^{\beta}]$. In the conventional cases of $\beta = 1$ (exponential) and $\beta = 2$ (superexponential), we found $E_0 = 17.7 \pm 2.8_{stat} \pm 5.0_{syst}$ GeV and $E_0 = 23.2 \pm 2.9_{stat} \pm 6.6_{syst}$ GeV, respectively. If instead we leave β as a free parameter, the best fit yields $E_0 = 20.4 \pm 3.9_{stat} \pm 7.4_{syst}$ GeV and $\beta = 1.2$.

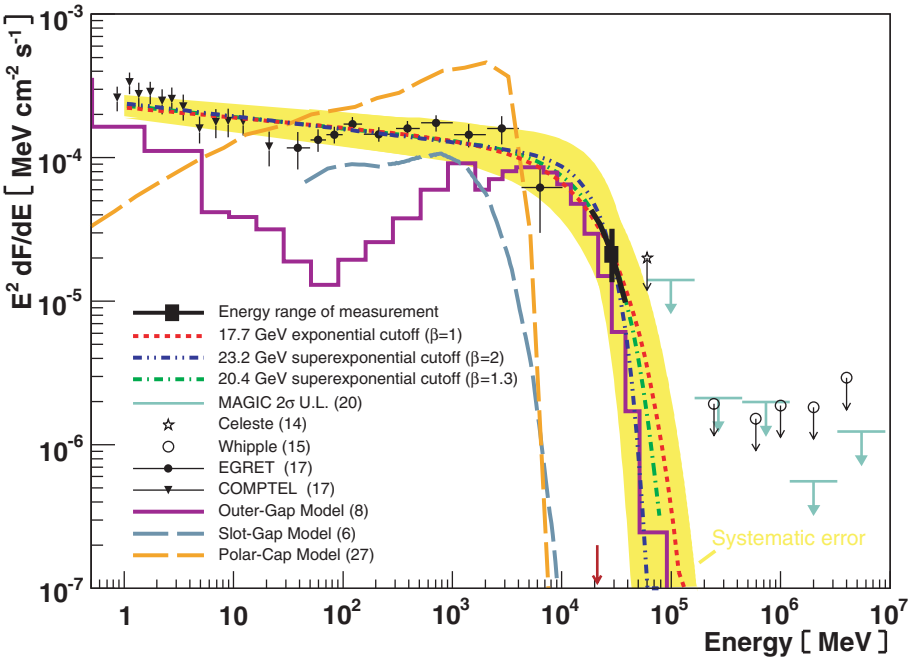

Fig. 4. Crab pulsar spectral cutoff. The solid circles and triangles on the left represent flux measurements from EGRET and COMPTEL (*17*). The arrows on the right denote upper limits from various previous experiments. We performed a joint fit of a generalized function $\{F(E) = A\,E^{-\alpha}\,exp[-(E/E_0)^{\beta}]\}$ to the MAGIC, EGRET, and COMPTEL data. The figure shows all three fitted functions for $\beta = 1$ (red line), $\beta = 2$ (blue line), and the best-fit, $\beta = 1.2$ (green line). The black line indicates the energy range, the flux, and the statistical error of our measurement. The yellow band illustrates the joint systematic error of all three solutions. The measurement is compared with three current pulsar models, a polar-cap model, a slot-gap model, and an outer-gap model. The sharp cutoff of the polar-cap (*27*) model is due to magnetic-pair production close to the surface of the neutron star. The slot-gap model (*6*) does not reach the observed cutoff energy, whereas the outer-gap (*8*) model can explain the high energy cutoff. The numbers in parentheses refer to the list of references.

The appropriate values for the Crab pulsar are $B_0 = 8 \times 10^{12}$ G (*8*), natural constant $B_{crit} = 4.4 \times 10^{13}$ G (*3*), and $P = 0.033$ s ($B_{crit} = 4.4$ E + 13 G is the critical field that marks the onset of quantum effects in a magnetized plasma). Using for E_{max} the superexponential cutoff energy $E_0 = 23.2 \pm 2.9_{stat} \pm 6.6_{syst}$ GeV, derived above for $\beta = 2$ as appropriate for the polar-cap scenario, one obtains $r/R_0 > 6.2 \pm 0.2_{stat} \pm 0.4_{syst}$; that is, the emitting region is located well above the NS surface. This result, however, contradicts the basic tenet of the polar-cap scenario (*1*–*3*) that particle acceleration and radiation emission do occur very close to the pulsar surface. This inconsistency rules out the polar-cap scenario for the Crab pulsar.

Our results therefore favor an outer-gap or slot-gap scenario for the Crab pulsar. For example, using in Eq. 1 the value of E_0 that corresponds to $\beta = 1$ (approximately consistent with the outer-gap picture), a high-altitude emitting region is inferred, which is fully consistent with the assumed scenario. Specific recent outer-gap (*8*, *9*) and slot-gap (*6*) predictions are compared with our data in Fig. 4. Although the former can provide emission of photons of energies as high as 25 GeV and hence explain our γ-ray data, the latter cannot. Thus, current outer-gap models seem preferred in explaining our measurement.

Lastly, our present measurements reveal a trend of P2/P1 increasing with energy: It is <0.5 at 100 MeV, ≈1 at 25 GeV, and >1 at 60 GeV (Fig. 2). This trend provides valuable information for theoretical studies that will further constrain the location of the emission region in the Crab pulsar's magnetosphere [for example, (*9*)].

References and Notes

1. M. A. Ruderman, P. G. Sutherland, *Astrophys. J.* **196**, 51 (1975).
2. J. K. Daugherty, A. K. Harding, *Astrophys. J.* **252**, 337 (1982).
3. M. G. Baring, *Adv. Space Res.* **33**, 552 (2004).
4. J. Arons, E. T. Scharlemann, *Astrophys. J.* **231**, 854 (1979).
5. A. G. Muslimov, A. K. Harding, *Astrophys. J.* **606**, 1143 (2004).
6. A. K. Harding, J. V. Stern, J. Dyks, F. Frackowiak, *Astrophys. J.* **680**, 1378 (2008).
7. K. S. Cheng, C. Ho, M. Ruderman, *Astrophys. J.* **300**, 500 (1986).
8. K. Hirotani, *arXiv*:0809.1283, (2008).
9. A. P. S. Tang, J. Takata, J. Jia, K. S. Cheng, *Astrophys. J.* **676**, 562 (2008).
10. γ-rays induce particle air showers in the atmosphere that emit Cherenkov light. The detection of this light allows measuring the energy and the direction of the incident γ-ray.
11. P. Chadwick *et al.*, *Astropart. Phys.* **9**, 131 (1998).
12. P. G. Edwards *et al.*, *Astron. Astrophys.* **291**, 468 (1994).
13. F. Aharonian *et al.*, *Astrophys. J.* **614**, 897 (2004).
14. M. de Naurois *et al.*, *Astrophys. J.* **566**, 343 (2002).
15. R. W. Lessard *et al.*, *Astrophys. J.* **531**, 942 (2000).
16. F. Aharonian *et al.*, *Astron. Astrophys.* **466**, 543 (2007).
17. L. Kuiper *et al.*, *Astron. Astrophys.* **378**, 918 (2001).
18. See the MAGIC telescope Web site; http://wwwmagic.mppmu.mpg.de.
19. A. N. Otte, thesis, Technical University, Munich (2007); available online at http://mediatum2.ub.tum.de/doc/620881/document.pdf.
20. J. Albert *et al.*, *Astrophys. J.* **674**, 1037 (2008).
21. The threshold of a Cherenkov telescope is usually defined as the peak in the energy distribution of triggered γ-ray events for a γ-ray source with an $E^{-2.6}$ power-law photon energy spectrum.
22. A. G. Lyne, R. S. Pritchard, F. Smith, *Mon. Not. R. Astron. Soc.* **265**, 1003 (1993).

23. R. W. Romani, *Astrophys. J.* **470**, 469 (1996).
24. P. Goldreich, W. H. Julian, *Astrophys. J.* **157**, 869 (1969).
25. Data provided by EGRET; ftp://legacy.gsfc.nasa.gov/compton/data/egret/.
26. F. Lucarelli *et al.*, *Nucl. Instr. Meth. A* **589**, 415 (2008).
27. A. K. Harding, private communication.

28. We thank the electronics division at the Max-Planck-Insitut, Munich, for their work in developing and producing the analog sum trigger system, especially O. Reimann, R. Maier, S. Tran, and T. Dettlaff. We also thank L. Stodolsky for comments. We acknowledge the Instituto de Astrofísica for providing all infrastructure on the Roque de los Muchachos in La Palma. The support of the German Bundesministerium für Bildung, Wissenschaft, Forschung und Technologie and Max-Planck-Gesellschaft, the Italian INFN and INAF, the Swiss Schweizerische Nationalfonds, and Spanish Ministerio de Ciencia e Innovación is acknowledged. This work was also supported by ETH research grant TH 34/043, by the Polish Ministertwo Nauki i Szkolnictwa Wyższego grant N N203 390834, and by the Young Investigators Program of the Helmholtz Gemeinschaft.

Supporting Online Material

www.sciencemag.org/cgi/content/full/1164718/DC1
SOM Text
Figs. S1 to S11
References

15 August 2008; accepted 8 October 2008
Published online 16 October 2008;
10.1126/science.1164718
Include this information when citing this paper.

List of authors and affiliations:

E. Aliu,[1] H. Anderhub,[2] L. A. Antonelli,[3] P. Antoranz,[4] M. Backes,[5] C. Baixeras,[6] J. A. Barrio,[4] H. Bartko,[7] D. Bastieri,[8] J. K. Becker,[5] W. Bednarek,[9] K. Berger,[10] E. Bernardini,[11] C. Bigongiari,[8]† A. Biland,[2] R. K. Bock,[7,8] G. Bonnoli,[12] P. Bordas,[13] V. Bosch-Ramon,[13] T. Bretz,[10] I. Britvitch,[2] M. Camara,[4] E. Carmona,[7] A. Chilingarian,[14] S. Commichau,[2] J. L. Contreras,[4] J. Cortina,[1] M. T. Costado,[15,16] S. Covino,[3] V. Curtef,[5] F. Dazzi,[8] A. De Angelis,[17] E. De Cea del Pozo,[18] R. de los Reyes,[4] B. De Lotto,[17] M. De Maria,[17] F. De Sabata,[17] C. Delgado Mendez,[15] A. Dominguez,[19] D. Dorner,[10] M. Doro,[8] D. Elsässer,[10] M. Errando,[1] M. Fagiolini,[12] D. Ferenc,[20] E. Fernandez,[1] R. Firpo,[1] M. V. Fonseca,[4] L. Font,[6] N. Galante,[7] R. J. Garcia Lopez,[15,16] M. Garczarczyk,[7] M. Gaug,[15] F. Goebel,[7] D. Hadasch,[5] M. Hayashida,[7] A. Herrero,[15,16] D. Höhne,[10] J. Hose,[7] C. C. Hsu,[7] S. Huber,[10] T. Jogler,[7] D. Kranich,[2] A. La Barbera,[3] A. Laille,[20] E. Leonardo,[12] E. Lindfors,[21] S. Lombardi,[8] F. Longo,[17] M. Lopez,[8]‡ E. Lorenz,[2,7] P. Majumdar,[7] G. Maneva,[22] N. Mankuzhiyil,[17] K. Mannheim,[10] L. Maraschi,[3] M. Mariotti,[8] M. Martinez,[1] D. Mazin,[1] M. Meucci,[12] M. Meyer,[10] J. M. Miranda,[4] R. Mirzoyan,[7] M. Moles,[19] A. Moralejo,[1] D. Nieto,[4] K. Nilsson,[21] J. Ninkovic,[7] N. Otte,[23,7]‡§ I. Oya,[4] R. Paoletti,[12] J. M. Paredes,[13] M. Pasanen,[21] D. Pascoli,[8] F. Pauss,[2] R. G. Pegna,[12] M. A. Perez-Torres,[19] M. Persic,[24] L. Peruzzo,[8] A. Piccioli,[12] F. Prada,[19] E. Prandini,[8] N. Puchades,[1] A. Raymers,[14] W. Rhode,[5] M. Ribó,[13] J. Rico,[1,25] M. Rissi,[2]‡ A. Robert,[6] S. Rügamer,[10] A. Saggion,[8] T. Y. Saito,[7] M. Salvati,[3] M. Sanchez-Conde,[19] P. Sartori,[8] K. Satalecka,[11] V. Scalzotto,[8] V. Scapin,[17] T. Schweizer,[7]‡ M. Shayduk,[7]‡ K. Shinozaki,[7] S. N. Shore,[26] N. Sidro,[1] A. Sierpowska-Bartosik,[18] A. Sillanpää,[21] D. Sobczynska,[9] F. Spanier,[10] A. Stamerra,[12] L. S. Stark,[2] L. Takalo,[21] F. Tavecchio,[3] P. Temnikov,[22] D. Tescaro,[1] M. Teshima,[7] M. Tluczykont,[11] D. F. Torres,[18,25] N. Turini,[12] H. Vankov,[22] A. Venturini,[8] V. Vitale,[17] R. M. Wagner,[7] W. Wittek,[7] V. Zabalza,[13] F. Zandanel,[19] R. Zanin,[1] J. Zapatero,[5] O.C. de Jager,[27]‖ E. de Ona Wilhelmi[1]‖¶

[1]Institut de Física d'Altes Energies, Edifici Cn, Campus Universitat Autònoma de Barcelona E-08193 Bellaterra, Spain. [2]Eidgenössische Technische Hochschule (ETH), Zürich CH-8093, Switzerland. [3]L'Istituto Nazionale di Astrofisica (INAF), I-00136 Rome, Italy. [4]Universidad Complutense, E-28040 Madrid, Spain. [5]Technische Universität Dortmund, D-44221 Dortmund, Germany. [6]Universitat Autònoma de Barcelona, E-08193 Bellaterra, Spain. [7]Max-Planck-Institut für Physik, D-80805 München, Germany. [8]Università di Padova and Istituto Nazionale di Fisica Nucleare (INFN), I-35131 Padova, Italy. [9]University of Lodz, PL-90236 Lodz, Poland. [10]Universität Würzburg, D-97074 Würzburg, Germany. [11]Deutsches Elektronen Synchrotron, D-15738 Zeuthen, Germany. [12]Università di Siena and INFN Pisa, I-53100 Siena, Italy. [13]Universitat de Barcelona, Institut de Ciencias del Cosmos (ICC)/Institut d'Estudis Espacials de Catalunya (IEEC), E-08028 Barcelona, Spain. [14]Yerevan Physics Institute, AM-375036 Yerevan, Armenia. [15]Instituto de Astrofísica de Canarias, E-38200, La Laguna,Tenerife, Spain. [16]Departamento de Astrofisica, Universidad, E-38206 La Laguna, Tenerife, Spain. [17]Università di Udine and INFN Trieste, I-33100 Udine, Italy. [18]IEEC–Consejo Superior de Investigaciones Cientificas (CSIC), E-08193 Bellaterra, Spain. [19]Instituto de Astrofisica de Andalucia (CSIC), E-18080 Granada, Spain. [20]University of California at Davis, Davis, CA 95616–8677, USA. [21]Tuorla Observatory, Turku University, FI-21500 Piikkiö, Finland. [22]Institute for Nuclear Research and Nuclear Energy, BG-1784 Sofia, Bulgaria. [23]Humboldt-Universität zu Berlin, D-12489 Berlin, Germany. [24]INAF/Osservatorio Astronomico and INFN, I-34143 Trieste, Italy. [25]Institució Catalana de Recerca i Estudis Avançats, E-08010 Barcelona, Spain. [26]Università di Pisa and INFN Pisa, I-56126 Pisa, Italy. [27]Unit for Space Physics, Northwest University, Potchefstroom 2520, South Africa.

†Present address: Instituto de Física Corpuscular, CSIC–Universitat de València, E-46071 Valencia, Spain.
‡To whom correspondence should be addressed. E-mail: tschweiz@mppmu.mpg.de (T.S.); nepomake@scipp.ucsc.edu (N.O.); Michael.Rissi@phys.ethz.ch (M.R.); shayduk@mppmu.mpg.de (M.S.); marcos.lopezmoya@pd.infn.it (M.L.M.)
§Present address: Santa Cruz Institute for Particle Physics, University of California, Santa Cruz, CA 95064, USA.
‖These authors are not members of the MAGIC Collaboration.
¶Present address: Astroparticule et Cosmologie, CNRS, Universite Paris, F-75205 Paris Cedex 13, France.

Ab Initio Determination of Light Hadron Masses

S. Dürr,[1] Z. Fodor,[1,2,3] J. Frison,[4] C. Hoelbling,[2,3,4] R. Hoffmann,[2] S. D. Katz,[2,3] S. Krieg,[2] T. Kurth,[2] L. Lellouch,[4] T. Lippert,[2,5] K. K. Szabo,[2] G. Vulvert[4]

More than 99% of the mass of the visible universe is made up of protons and neutrons. Both particles are much heavier than their quark and gluon constituents, and the Standard Model of particle physics should explain this difference. We present a full ab initio calculation of the masses of protons, neutrons, and other light hadrons, using lattice quantum chromodynamics. Pion masses down to 190 mega–electron volts are used to extrapolate to the physical point, with lattice sizes of approximately four times the inverse pion mass. Three lattice spacings are used for a continuum extrapolation. Our results completely agree with experimental observations and represent a quantitative confirmation of this aspect of the Standard Model with fully controlled uncertainties.

The Standard Model of particle physics predicts a cosmological, quantum chromodynamics (QCD)–related smooth transition between a high-temperature phase dominated by quarks and gluons and a low-temperature phase dominated by hadrons. The very large energy densities at the high temperatures of the early universe have essentially disappeared through expansion and cooling. Nevertheless, a fraction of this energy is carried today by quarks and gluons, which are confined into protons and neutrons. According to the mass-energy equivalence $E = mc^2$, we experience this energy as mass. Because more than 99% of the mass of ordinary matter comes from protons and neutrons, and in turn about 95% of their mass comes from this confined energy, it is of fundamental interest to perform a controlled ab initio calculation based on QCD to determine the hadron masses.

QCD is a generalized version of quantum electrodynamics (QED), which describes the electromagnetic interactions. The Euclidean Lagrangian with gauge coupling g and a quark mass of m can be written as $\mathcal{L} = -1/(2g^2)\mathrm{Tr}F_{\mu\nu}F_{\mu\nu} + \overline{\psi}[\gamma_\mu(\partial_\mu + A_\mu) + m]\psi$, where $F_{\mu\nu} = \partial_\mu A_\nu - \partial_\nu A_\mu + [A_\mu, A_\nu]$. In electrodynamics, the gauge potential A_μ is a real valued field, whereas in QCD it is a 3×3 matrix field. Consequently, the commutator in $F_{\mu\nu}$ vanishes in QED but not in QCD. The ψ fields also have an additional "color" index in QCD, which runs from 1 to 3. Different "flavors" of quarks are represented by independent fermionic fields, with possibly different masses. In the work presented here, a full calculation of the light hadron spectrum in QCD, only three input parameters are required: the light and strange quark masses and the coupling g.

The action S of QCD is defined as the four-volume integral of $\mathcal{L}$. Green's functions are averages of products of fields over all field configurations, weighted by the Boltzmann factor $\exp(-S)$. A remarkable feature of QCD is asymptotic freedom, which means that for high energies (that is, for energies at least 10 to 100 times higher than that of a proton at rest), the interaction gets weaker and weaker (*1*, *2*), enabling perturbative calculations based on a small coupling parameter. Much less is known about the other side, where the coupling gets large, and the physics describing the interactions becomes nonperturbative. To explore the predictions of QCD in this nonperturbative regime, the most systematic approach is to discretize (*3*) the above Lagrangian

[1]John von Neumann–Institut für Computing, Deutsches Elektronen-Synchrotron Zeuthen, D-15738 Zeuthen and Forschungszentrum Jülich, D-52425 Jülich, Germany. [2]Bergische Universität Wuppertal, Gaussstrasse 20, D-42119 Wuppertal, Germany. [3]Institute for Theoretical Physics, Eötvös University, H-1117 Budapest, Hungary. [4]Centre de Physique Théorique (UMR 6207 du CNRS et des Universités d'Aix-Marseille I, d'Aix-Marseille II et du Sud Toulon-Var, affiliée à la FRUMAM), Case 907, Campus de Luminy, F-13288, Marseille Cedex 9, France. [5]Jülich Supercomputing Centre, FZ Jülich, D-52425 Jülich, Germany.

ERRATUM

Post date 20 March 2009

Reports: "Observation of pulsed γ-rays above 25 GeV from the Crab pulsar with MAGIC" by The MAGIC Collaboration (21 November 2008, p. 1221). The e-mail address for N. Otte was incorrect. The correct address is nepomuk@scipp.ucsc.edu.